# EXPERIMENTAL OBSERVATIONS ON THE BEHAVIOR OF A PILED RAFT FOUNDATION

**Dr. Mosa J. Al-Mosawi[(1)]** **Dr. Mohammed Y. Fattah[(2)]**
**Abbas A. O. Al-Zayadi[(3)]**

(1) Professor, College of Engineering, Civil Eng. Dept., University of Baghdad, Iraq.
(2) Assistant Professor, Building and Construction Eng. Dept., University of Technology.
(3) Formerly graduate student, College of Engineering, Civil Eng. Dept, University of Baghdad.

**ABSTRACT**
The piled raft is a geotechnical composite construction consisting of three elements: piles, raft and soil. In the design of piled rafts, the load shared between the piles and the raft, and the piles are used up to a load level that can be of the same order of magnitude as the bearing capacity of a comparable single pile or even greater. Therefore, the piled raft foundation allows reduction of settlements in a very economic way as compared to traditional foundation concepts.

This paper presents experimental study to investigate the behavior of piled raft system in sandy soil. A small scale "prototype" model was tested in a sand box with load applied to the system through a compression machine. The settlement was measured at the center of the raft, strain gages were used to measure the strains and calculate the total load carried by piles. Four configurations of piles (2x1, 3x1, 2x2 and 3x2) were tested in the laboratory, in addition to rafts with different sizes. The effects of pile length, pile diameter, and raft thickness on the load carrying capacity of the piled raft system are included in the load-settlement presentation.

It was found that the percentage of the load carried by piles to the total applied load of the groups (2x1, 3x1, 2x2, 3x2) with raft thickness of 5 mm, pile diameter of 9 mm, and pile length of 200 mm was 28% , 38% , 56% , 79% , respectively. The percent of the load carried by piles increases with the increase of number of piles.

# مشاهدات عملية على تصرف الأساس الحصيري المستند الى ركائز

**الخلاصة:**
يعتبر الأساس الحصيري المستند الى ركائز منشأ جيوتقنيا مركبا يتألف من ثلاثة عناصر هي الركائز و الحصيرة و التربة. عند تصميم الأسس الحصيرية المستندة الى ركائز تحصل مشاركة في الحمل بين الركائز و الحصيرة و تصمم الركائز لمستوى حمل يمكن أن يكون مساويا الى مقدار قابلية تحمل الركيزة المنفردة و ربما أكبر. و لذلك فان الأساس الحصيري المستند الى ركائز يسمح بتقليل الهبوط بطريقة اقتصادية مقارنة مع مبادئ تصميم الأسس التقليدية.

هذا البحث يعرض دراسة عملية لتحري تصرف منظومة الأساس الحصيري المستند الى ركائز في ترب رملية، حيث تم فحص نموذج مختبري مصغر في صندوق من الرمل ، و تم تسليط الحمل على المنظومة من خلال ماكنة الضغط. و قد قيس الهبوط في مركز الحصيرة فيما أستعملت مقاييس انفعال لقياس الانفعالات و حساب الحمل الكلي الذي تتحمله الركائز. و فحصت مختبريا أربعة أشكال لمجاميع الركائز (1x2 و 1x3 و 2x2 و 2x3) و ذلك باستعمال ركائز ذات أحجام مختلفة. و درس تأثير كل من طول الركائز و قطرها و سمك الحصيرة على قابلية تحمل منظومة الحصيرة المستندة الى ركائز من خلال عرض علاقات الحمل – الهبوط.

و قد وجد أن نسبة الحمل الذي تحمله الركائز من الحمل المسلط على مجاميع الركائز(1x2 و 1x3 و 2x2 و 2x3) عندما يكون سمك الحصيرة 5 ملم و قطر الركيزة 9 ملم و طولها 200 ملم تبلغ 28% و 38% و 56% و 79% على التوالي، و تتزايد نسبة الحمل الذي تحمله الركائز مع زيادة عدد الركائز.

## INTRODUCTION

Raft and pile groups are the two alternative foundation options to support structures with heavy column loads. Raft is normally designed as rigid in order to withstand high moment and differential settlement, which is a function of intensity of load and relative stiffness of raft and soil. In the case of pile groups more number of piles is provided than required to cater the column load and to practically eliminate the settlement, which makes the foundation to be very expensive. The concept of pile raft was conceived and introduced about three decades back to overcome the difficulties stated above as well as for the effective utilization of the pile group.

A piled foundation system consists of three elements: raft, piles, and the subsoil. An external vertical load $Q$ is equilibrated partly by the contact pressure between the raft and the soil (with resultant $Q_R$), and partly by the piles (with resultant $Q_G$). It is then possible to introduce a coefficient,

$$\alpha_P = \frac{Q_G}{Q} \qquad (1)$$

where $\alpha_P$ represents the portion of the load taken by the piles.

The case $\alpha_P$ = 0 represents a shallow foundation with no piles (or raft foundation), while the case $\alpha_P$=1 represents a pile group with a raft clear from the ground. Piled raft foundations cover the range 0 < $\alpha_P$<1. Every piled foundation behaves like a piled raft, with the exception of those cases where there is no contact between the raft and the soil as in offshore structures (de Sanctis and Mandolini, 2006).

Piled raft foundations are composite structures unlike classical foundation where the building load is either transferred by the raft or the piles alone. In a piled raft foundation, the contribution of the piles as well as the raft is taken into account.

The piles transfer a part of the building loads into deeper and stiffer layers of soil and thereby allow the reduction of settlement and differential settlement in a very economic way. Piles are used up to a load level which can be of the same order of magnitude as the bearing capacity of a comparable single pile or even greater (Hartmann and Jahn, 2001).

The adoption of piled raft foundations concept in the design of pile groups is by no means new, and has been described by several authors, including Zeevaert (1957), Davis and Poulos (1972), Hooper (1973), Burland et al. (1977), Katzenbach and Reul (1997), Prakoso and Kulhawy (2000), and Reul and Randolph (2003), among many others. In the early years, because of the limited availability of computers memory and processing speed, the use of numerical methods was confined to simple problems. In the last two decades due to the rapid development in computer technologies, numerical methods such as full three-dimensional methods are often used to solve complex problems.

## EXPERIMENTAL WORK

Laboratory-scale investigations into piles behavior remain popular because of the high cost of field testing and the possibility of achieving specific soil characteristics in a laboratory environment. The monitored

behavior of prototype structures has led to a better understanding of piles foundation and enables more reliable and economical design to be employed.

Model tests are relatively inexpensive and can be conducted under controlled laboratory conditions. This provides an efficient means of investigation. For instance, Cox et al. (1984) reported a study in which tests on 58 single piles and 41 pile groups were performed. They varied the geometric arrangement of piles within groups, the number of piles per group, and the spacing between piles (Mokwa, 1999).

The main purpose of the experimental research implemented in this paper is to study the load sharing mechanism between raft and piles, as well as the load settlement behavior of piled raft with different configurations, lengths of piles, and diameters. The following sections describe the test setup used to perform the model tests, the mechanical properties of the investigated soil, the configuration of model piled rafts, and the testing program and procedure. All the experimental works have been made in the laboratory of soil mechanics in the University of Baghdad.

**Test Setup**

All model tests were conducted using the setup shown in **Figure (1)**, which consists of a soil tank, model piled raft and loading machine. The vertical load was applied to the model piles by means of 10 ton compression test machine (Wykeham Farrance, England). It is a displacement controlled machine with rate capability in the range of (0.0001–59.99 mm/min), during all the experimental tests, the loading rate was kept constant with a value of 1 mm/min. The applied load was measured using a proving ring (Wykeham Farrance, England) of 5 kN and 10 kN capacity with 0.00434 and 0.00606 kN accuracy, respectively. A deformation dial gauge with 0.01 mm sensitivity was used for measuring displacements at the centerline of the piled raft model. Strain gages were adhered to the pile and connected to a strain indicator so as to measure the strains in the pile.

**Soil Tank**

The soil tank has 0.6 m length, 0.6 m width, and 0.7 m height supported by a relatively rigid steel framework stiffened with 3 lines of 25 mm steel angles, provided with a 0.28 x 0.22 m hatch for sand unloading. The base was stiffened with additional 3mm steel plates and 25mm steel angle frame and stiffeners, in order to prevent concentration of the load exerted from the position on a small area. The dimensions of the tank were chosen so that the tank can be put inside the testing machine and there will be no interference between the walls of the soil tank and the failure zone around the piled raft system. The internal sides of the tank were covered with polyethylene sheets in order to minimize friction that may develop between the steel tank surfaces and the soil. **Figure (2)** presents the soil tank fitted inside the compression machine.

**Soil Properties**

The soil used for the model tests is clean, oven-dried, uniform quartz (Kerbela) sand. The tests are performed on medium dense sand with maximum and minimum dry unit weights of the sand determined according to the ASTM (D4253-2000) and ASTM (D4254-2000) specifications, respectively. The specific gravity test is performed according to ASTM (D854-2005) and the grain size distribution is analyzed according to ASTM (D422-2001) specifications. **Figure (3)** shows the grain size distribution of the sand and Table (1) shows the physical properties of the tested sand. The angle of internal friction is determined using the direct shear test and found to be 38°.

**Sand Deposit Preparation**

The sand deposit was prepared using the sand raining technique. A special raining device similar to that recommended by Bieganousky and Marcuson (1976) was designed to obtain a uniform deposit with the desired density; this

devise has been used by previous researchers (Al-Jebouri, 1986, and Jawad 2009). **Figure (2)** shows a schema for the raining device.

**Table** (1), Physical properties for the tested sand.

| Property | Value |
|---|---|
| Grain size analysis | |
| Effective size, $D_{10}$ | 0.26 mm |
| Coefficient of uniformity, $C_u$ | 2.67 |
| Coefficient of curvature, $C_c$ | 1.0 |
| Classification (USCS)* | SP |
| Specific gravity, $G_s$ | 2.63 |
| Dry unit weights | |
| Maximum unit weight, $\gamma_{d\,(max)}$ | 17.5 kN/m$^3$ |
| Minimum unit weight, $\gamma_{d\,(min)}$ | 14.50 kN/ m$^3$ |
| Test unit weight, $\gamma_{d\,(test)}$ | 16.30 kN/ m$^3$ |
| Relative density, $D_r$ | 63% |
| Void ratio | |
| Maximum void ratio, $e_{max}$ | 0.82 |
| Minimum void ratio, $e_{min}$ | 0.50 |
| Test void ratio, $e_{test}$ | 0.62 |

* USCS refers to Unified Soil Classification System

The unit weight of the sand deposit in the raining method depends primarily on the drop height and the discharge rate of the sand (Turner and Kulhawy, 1987). The `height of the free fall of the sand can be controlled by adjusting the elevation of the raining device with respect to the sand tank while the discharge rate of the sand was kept constant.

Sand deposits were prepared with the sand tank resting on the loading platen of the testing machine so that the sand deposit was not disturbed and hence the desired unit weight of the sand is not altered.

Calibration curves similar to those prepared by Al-Jebouri (1986) to find the proper drop height related to the density, void ratio and relative density for maintaining a constant density of sand during all the experimental tests were made in this work. **Figure (4)** shows these calibration curves. The height of drop was chosen to be 50 cm, which corresponds to a placing unit weight of 16.3 kN/m$^3$ and a void ratio of 0.63 and a relative density of 63%.

## Model Piled Rafts

The model piles used in this study are smooth aluminum pipe piles having three different outside diameters and thicknesses. The embedment (depth to diameter) ratio $l/d$ = 20, 25, and 30, where $l$ represents the pile length and $d$ is the outside diameter of the pipe pile. The spacing between piles is kept constant (S = 5 cm) in all tests.
model raft used in the test was also made of aluminum with The smooth surface and two different thicknesses 5 and 2.5 mm to study the effect of raft stiffness. Both piles and rafts were composed of ALUPCO alloy, which is supplied locally by ALUPCO Alloys Company. The technical specification and the mechanical properties of the used alloy are shown in table (2).

**Table** (2), Mechanical properties of the used Aluminum alloy.

| Property | Value |
|---|---|
| Minimum yield strength (N/mm$^2$) | 160 |
| Minimum ultimate strength (N/mm$^2$) | 215 |
| Minimum % of elongation | 10 |
| Poisson's ratio | 0.34 |

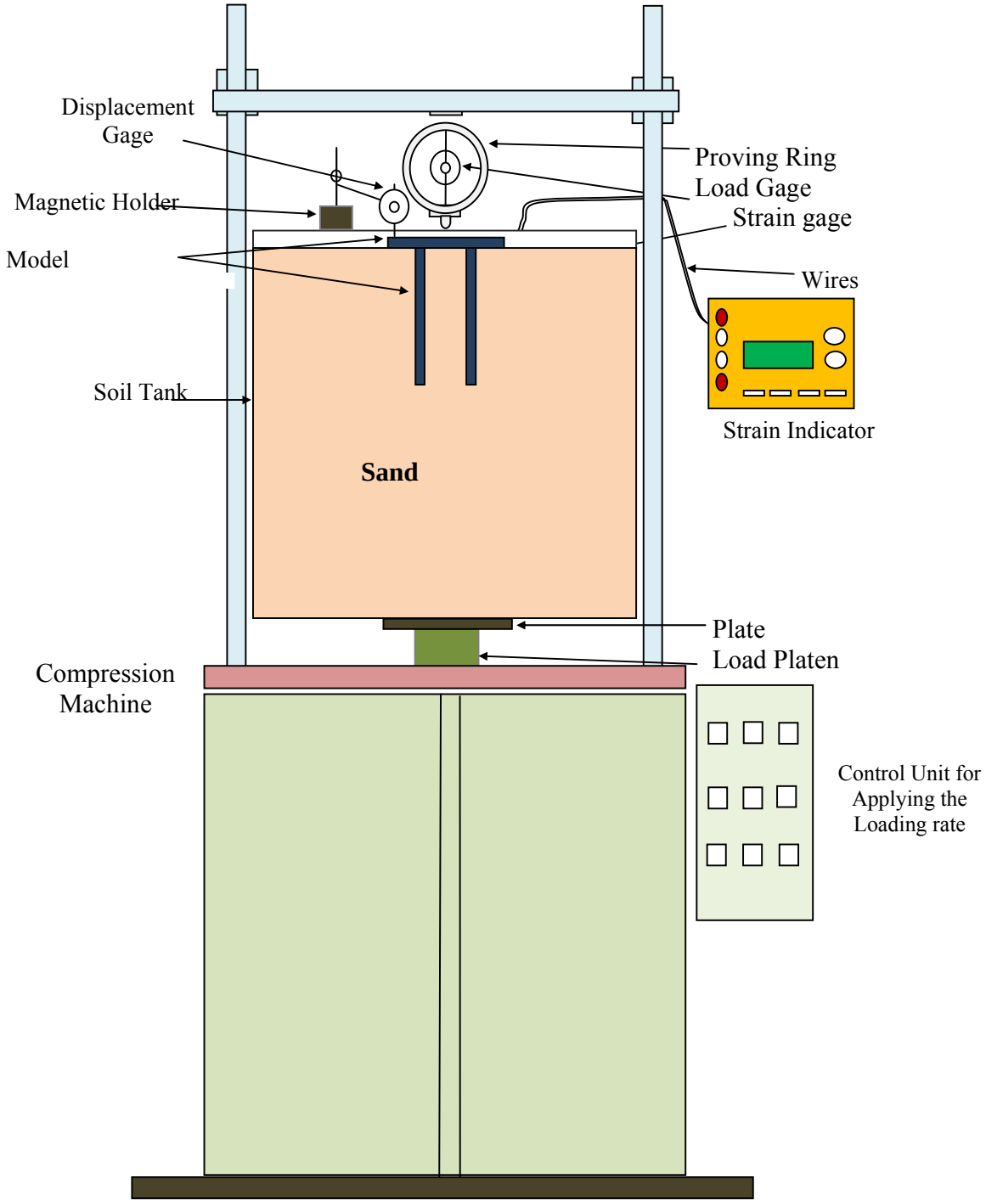


**Fig.** (1), Setup of the laboratory model.


a. Soil tank used in the experimental study.

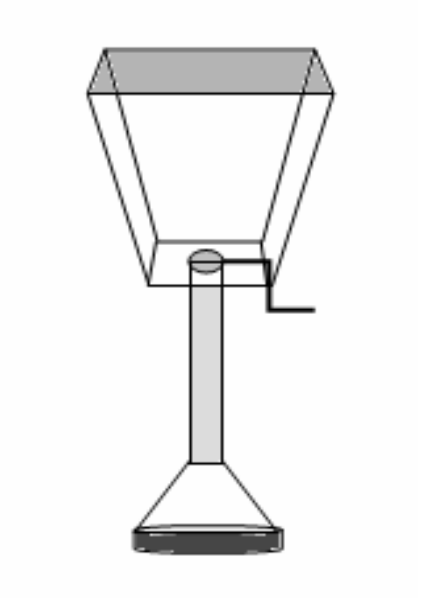

b. Sand hopper used in the raining technique.

**Fig.** (2), Test equipment.

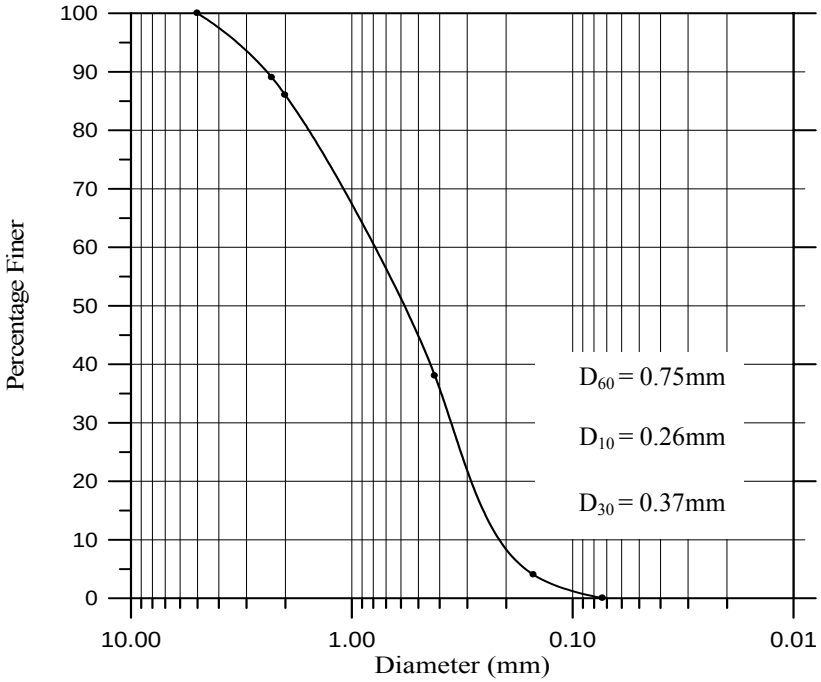


**Fig.** (3), Grain size distribution of the sand.

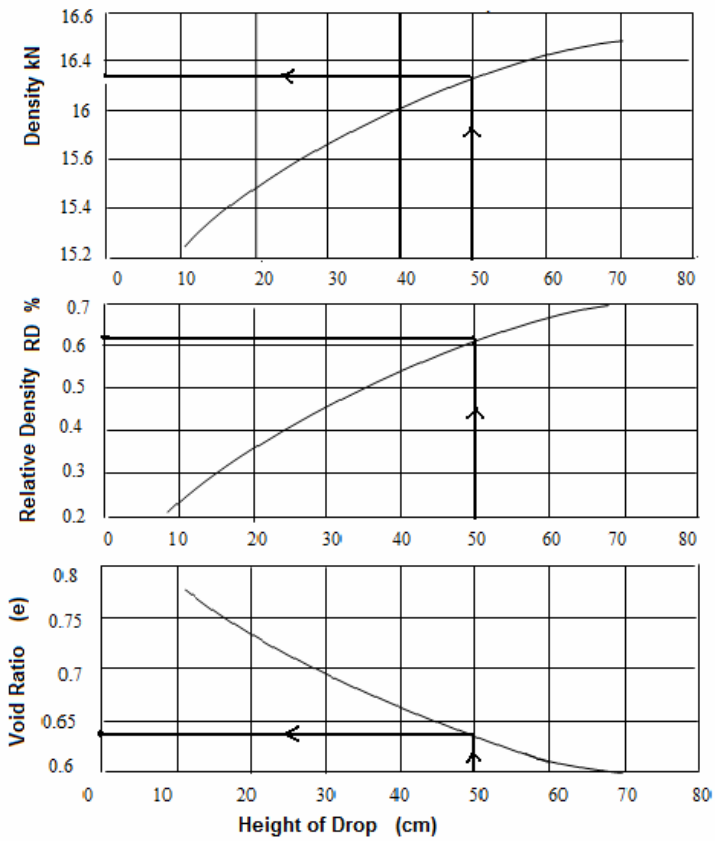


**Fig.** (4), Density calibration curves.

A laboratory test was carried out to find the modulus of elasticity for an Aluminum

sample making use of the strain gage technique. A stress strain relationship was obtained in the laboratory from which the modulus of elasticity of the Aluminum was found to be 65 GPa.

A strain gage produced by Vishay Micro-Measurements was attached to the pile shaft and connected to a strain indicator to read the strain in the pile. Since the modulus of elasticity and the cross sectional area of the piles are known, then the amount of load carried by pile can be obtained. The load sharing mechanism between piles and raft can be well studied.

**Strain Indicator**

A 3800 Wide-Range Strain Indicator was used to read the strain initiated in the piles. This electronic instrument is highly versatile, specifically designed for use with strain gages. Its unique combination of "wide-range" features and easy-to- use controls makes the Model 3800 the right choice for many strain gage and transducers measurement applications.

The strain indicator of the model 3800 shown in **Figure (5)** can be used to obtain extremely accurate, high resolution strain measurements in a variety of circumstances. Resolutions of 0.10 με (micro strain) are routinely possible if the excitation voltage kept above 5.0V, even higher resolution can be kept in the 10 to 15V range and the operation environment is relatively noise-free.

The used strain indicator was utilized with shunt calibration resistors across the internal $120\Omega$ and $350\Omega$ dummy gages for quarter bridge calibration. The calibration resistors can be used in conjunction with the gage factor potentiometer to compensate for leadwire resistance (Model 3800 Manual, 2002).

Before adopting the results obtained from the strain indicator, an external calibration was made by testing a steel bar with known modulus of elasticity twice, once by using the 3800 Vishay Model and then by using DMD-21 OMEGA strain indicator which was used only for the calibration purposes. The results of the two strain indicators were exactly the same, and the same modulus of elasticity of steel was obtained by the two devices.

**TESTING PROCEDURE**

The procedure followed in testing the piled raft model was divided into the following steps:

**I. Building the piled raft model:**
Aluminum pipe piles with different diameters and lengths, forming four configurations 2x1, 3x1, 2x2, and 3x2, were prepared to fulfill the testing program of the experimental study. The piles were fixed to approximately rigid rafts using strong epoxy. The epoxy was used as substitution for welding the piles to the raft since the aluminum may melt in the extremely high temperature of welding. The epoxy simulates a semi-fixed connection of piles to the raft.

**II. Attachment of strain gage:**
A strain gage was placed in the middle of the pile shaft**.** The strain gage was covered with a thin layer of sponge to protect it from damage, at the same time sponge does not bear any load.

**III. Preparation of sand deposit and placing of piled raft model:**
The sand was placed in the tank according to the raining techniques, i.e. maintaining a dropping height of 50 cm. After each test, the sand box should be emptied to a depth below the zone of influence (which was considered as 2L below the raft, where L is the pile length). During the process of sand raining, the piled raft model was placed at the center of the tank and under the loading ring, a bubble balance was used to insure

the level of the raft, then the raining was continued to a level of the lower surface of the raft. The final layer of the sand is leveled by a sharp edge ruler.

## IV. Connection of wires to the strain indicator:

A quarter bridge connection was performed in the use of strain indicator, a gage factor of 2.03, excitation voltage of 10V and shunt calibration resistor of 120Ω was used to compensate for the leadwire resistant. Before starting the test, a reading of 0.00 was set in the strain indicator and waiting for 5 minutes to allow the system to be stable, then if the reading still around 0.00, the test can be started successfully.


**Fig.** (5), Visahy 3800 strain indicator.

**Testing Program**

A program for performing a parametric study on piled raft model was carried out by testing four configurations with the same pile length (200 mm), diameter (12 mm), spacing (50 mm) and two raft thicknesses of 5 mm and 2.5 mm). The results were compared with rafts of the same sizes and thicknesses.

The effect of increasing the diameter of the pile as well as the effect of pile length on the load settlement and load sharing have been studied by considering three pile diameters (9, 12 and 15 mm) and three pile lengths (200, 250 and 300 mm), while keeping the raft thickness constant (5 mm) and the configuration also was constant (2x2 group). For studying the effect of raft stiffness, two raft thicknesses were considered for a 2x2 group of piles and 200 mm, 12 mm pile length and diameter, respectively.

## V. Application of vertical load:

A vertical load was applied through a 5 or 10 kN proving ring, a constant loading rate of 1 mm/min was adopted in the entire testing program. The test was continued until recording a continuous displacement of the piled raft under constant load. The load was read from a dial gage fixed to the proving ring, while the central displacement of the raft was read by a dial gage of 0.01 mm sensitivity, and the strain in the pile was read from the strain indicator.

The above steps were repeated for each test. **Figure (6)** shows a piled raft model ready to be tested.

## PRESENTATION AND DISCUSSION OF THE EXPERIMENTAL RESULTS

The load applied to the center of the model raft is transmitted partly to the soil and another part is transmitted to the piles. The percent of load

carried by piles to the total applied load can be determined in the laboratory through instrumentation of the piles with strain gages to find out the strain initiated in each pile. Due to the limited capabilities of the measuring devices in the laboratory, strain can be measured in only one pile in the group. To overcome this lack of devices, rigid rafts have been used to distribute the load equally to the piles, and by knowing the load in one pile, the total load carried by other piles can be obtained. By knowing the strain in a pile, one can calculate the load in that pile if the cross sectional area and the modulus of elasticity are known.

(a) Model piled raft with attached strain gage.

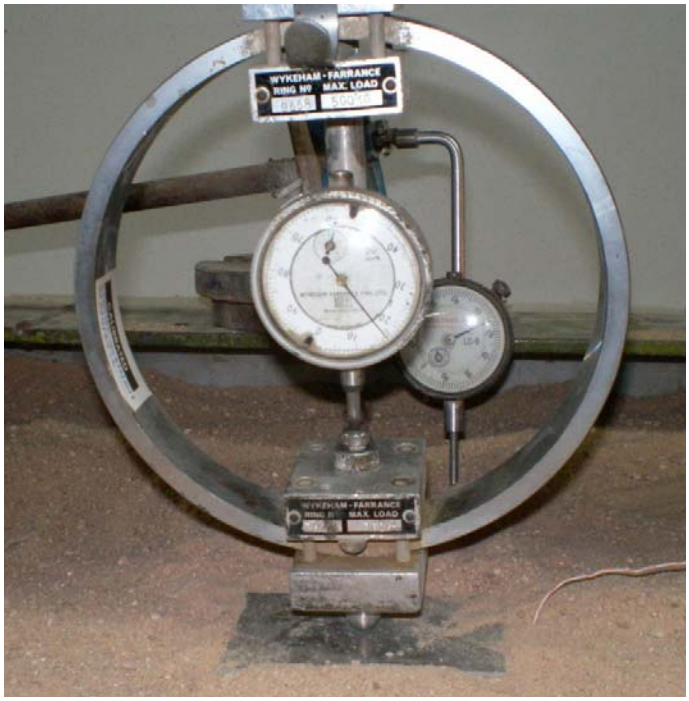


(b) Model piled raft and proving ring.

**Fig.** (6), Model piled raft ready to test.

**Configurations of Piled Rafts**

Piled raft configurations used maintain symmetrical shapes, especially where the differential settlement is expected to be of no major concern. Four different configurations of piles are used in the piled raft prototypes. The groups consist of (2x1), (3x1), (2x2) and (3x2) piles, a schematic diagram for the groups is shown in **Figure (7)**.

**Load Carrying Capacity of Rafts and Piled Rafts**

This section presents the load carrying capacity of the piles in each group as well as the load settlement behavior of the whole system with outside diameters having the values of 9, 12 and 15 mm, keeping the length of piles constant at 200 mm.

In the following figures, the settlement is plotted with the vertical applied load. In the same figures a curve representing the load settlement behavior of unpiled raft is added, where rafts are tested separately for the sake of comparison. The total load carried by piles is also shown in the same figure as calculated from strains measured through the use of strain gages.

**Figures (8) to (10)** show the load settlement behavior of piled rafts, and rafts of the same size and thicknesses and dimensions as well as the load carried by piles for the group of (2x1) with three different diameters (9, 12 and 15 mm), respectively. The pile length is kept constant (200 mm). **Figures (11) to (13)** are devoted for the groups of (3x1), while **Figures (14) to (16)** represent the groups of (2x2) piles. For the group of (3x2) only, one case having a pile diameter of (9 mm) and length of pile (200 mm) is shown in **Figure (17)**.

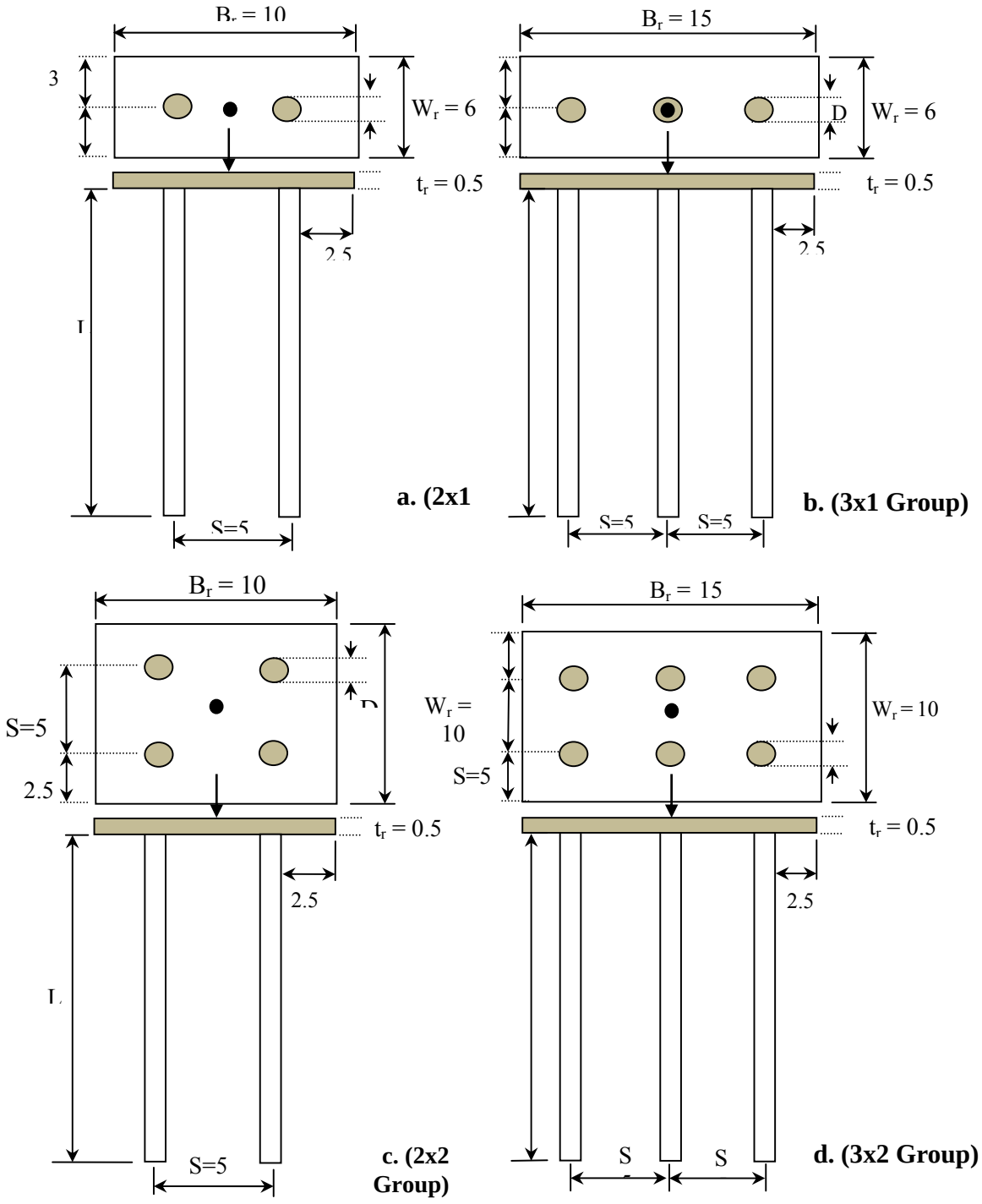


*Note: All dimensions are in cm.

**Fig. (7),** Piled raft configurations adopted in the experimental research.

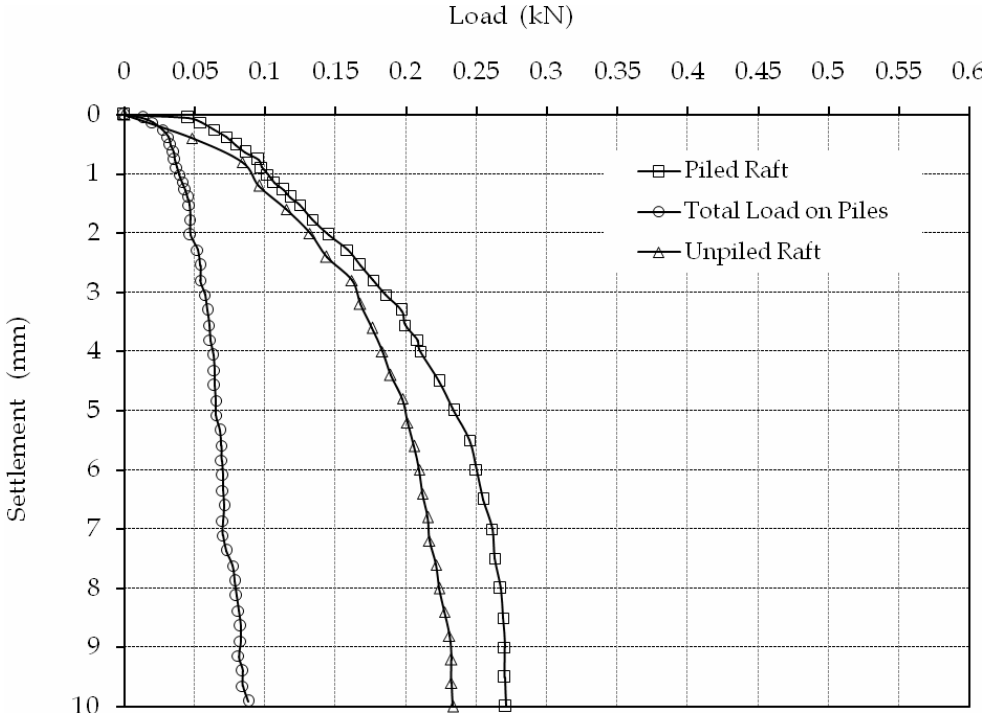


**Fig. (8)** Load –displacement curve for (**2x1**) piled raft, unpiled raft and total load on piles (L=200 mm, D=9 mm).

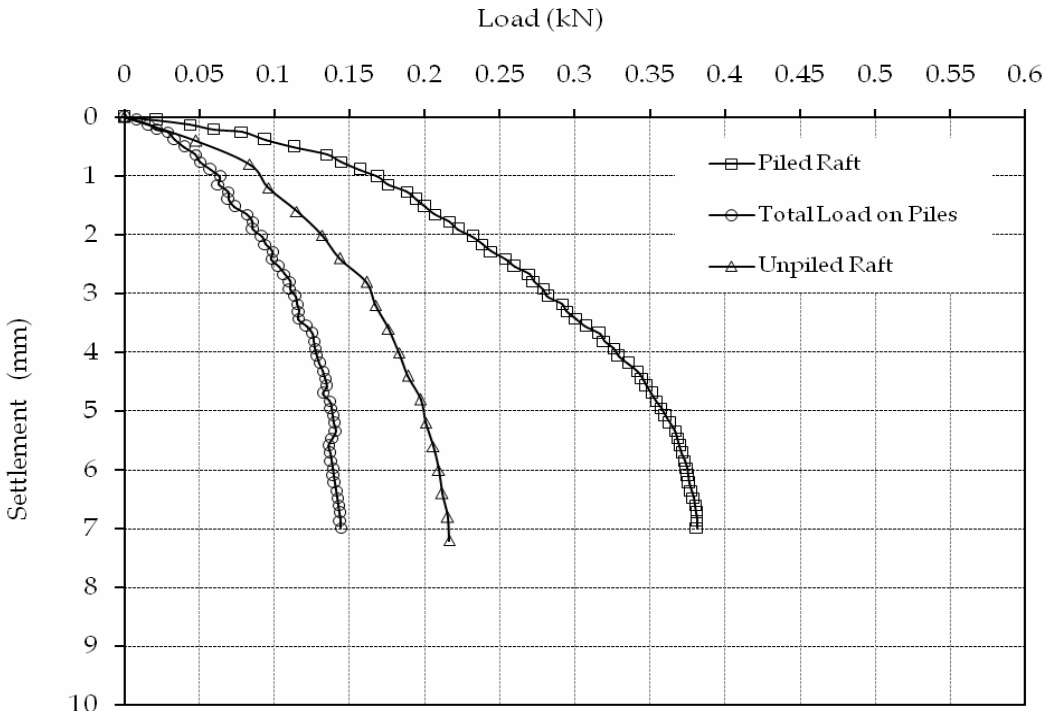


**Fig. (9)** Load – displacement curve for (**2x1**) piled raft, unpiled raft and total load on piles (L=200 mm and D=12 mm).

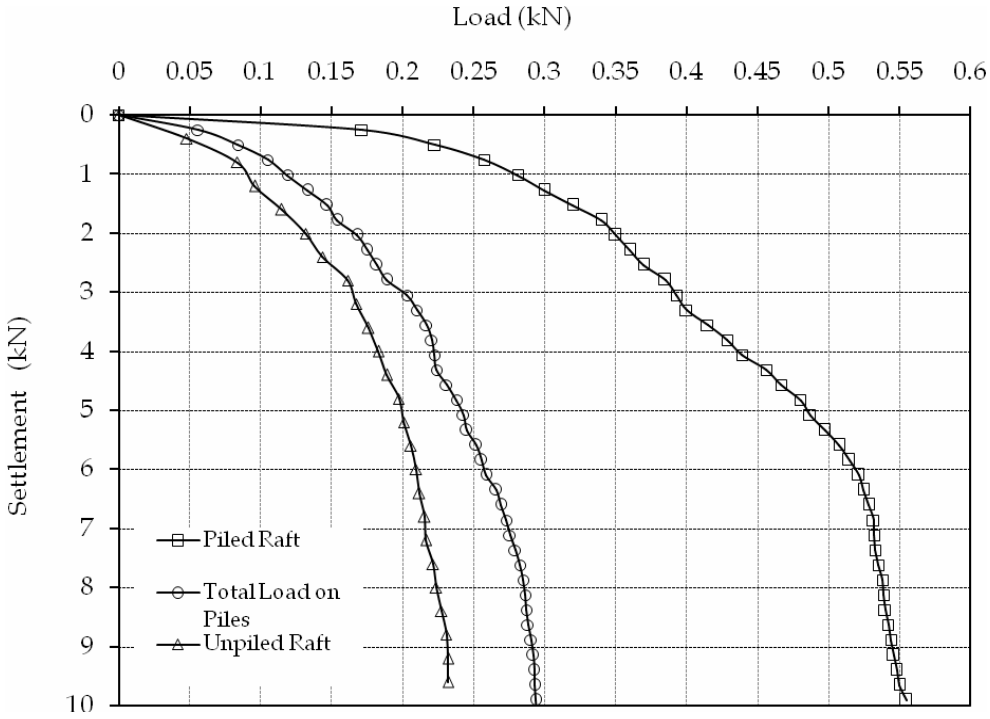


**Fig. (10)** Load – displacement curve for (**2x1**) piled raft, unpiled raft and total load on piles (L=200 mm and D=15 mm).

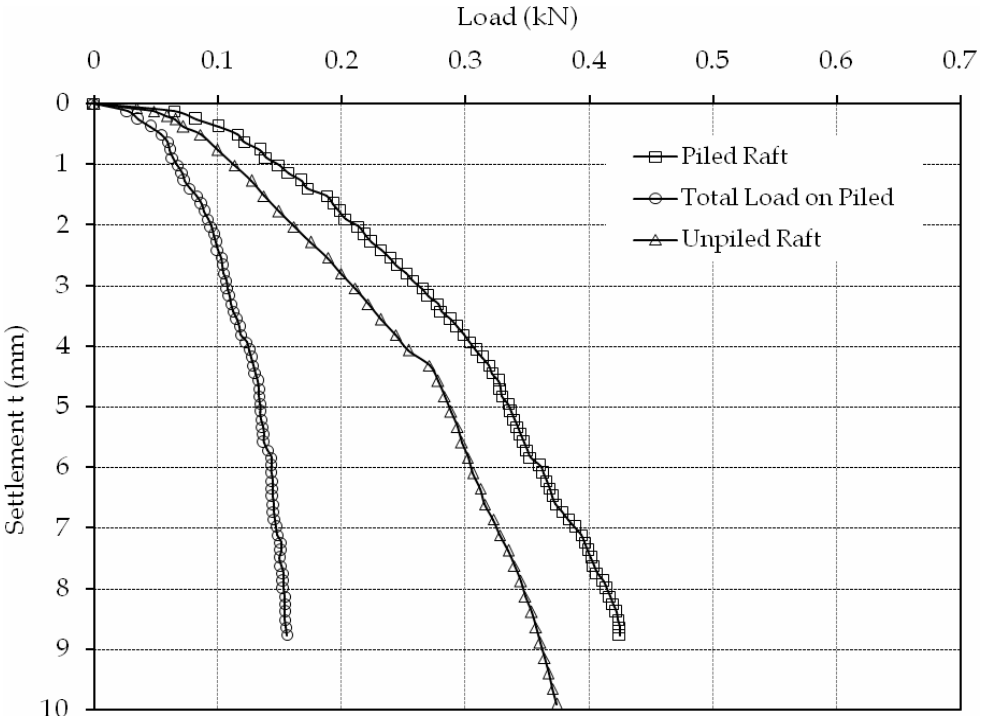


**Fig. (11)** Load – displacement curve for (**3x1**) piled raft, unpiled raft and total load on piles (L=200 mm, D=9 mm).

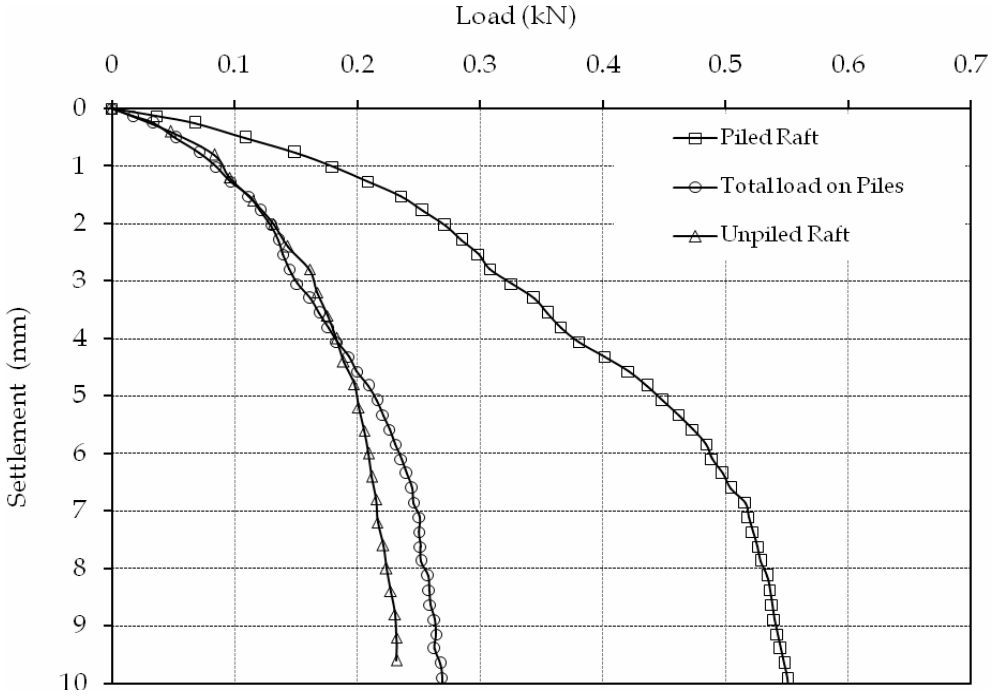


**Fig. (12)** Load – displacement curve for (**3x1**) piled raft, unpiled raft and total load on piles (L=200mm, D=12 mm).

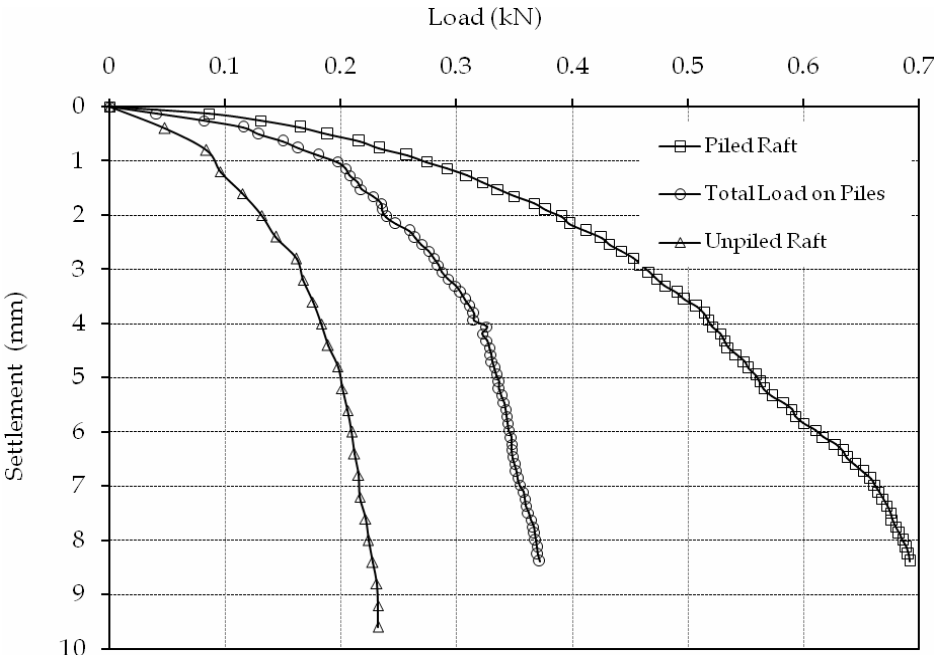


**Fig. (13)** Load – displacement curve for (**3x1**) piled raft, unpiled raft and total load on piles (L=200 mm, D=15 mm).

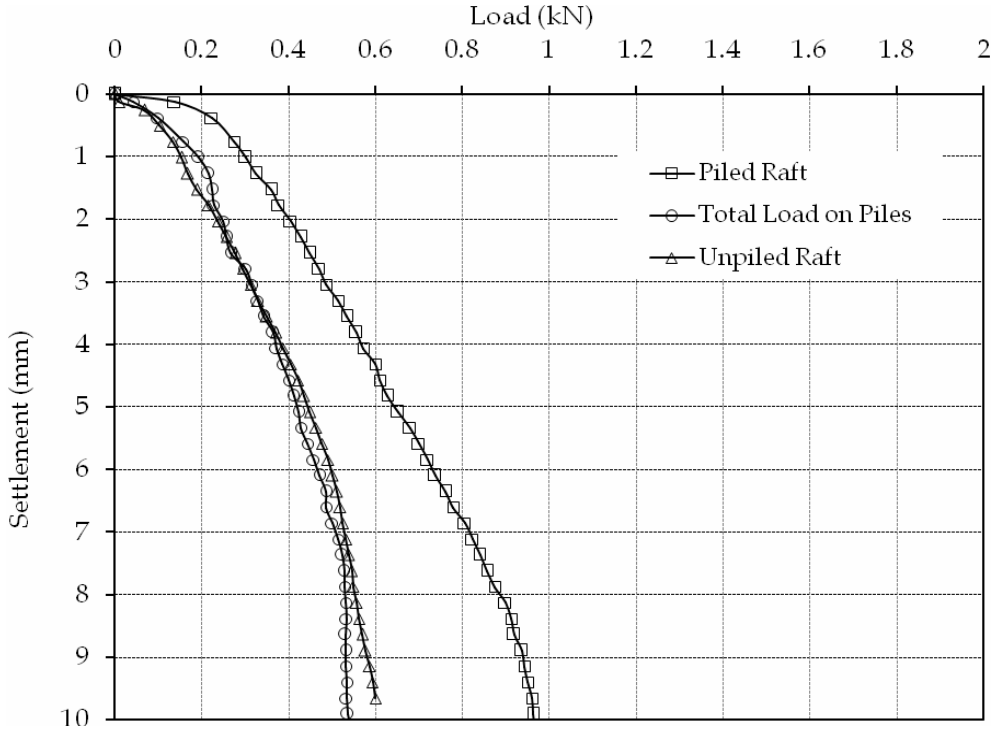


**Fig. (14)** Load – displacement curve for (**2x2**) piled raft, unpiled raft and total load on piles (L=200 mm, D=9 mm).

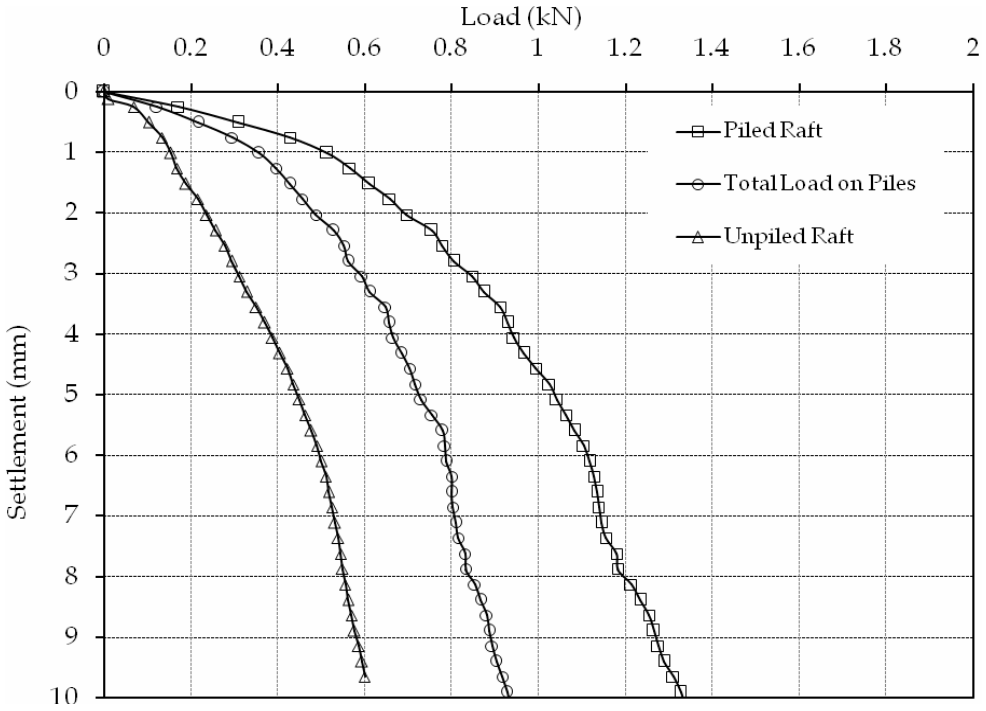


**Fig. (15)** Load – displacement curve for (**2x2**) piled raft, unpiled raft and total load on piles (L=200 mm and D=12 mm).

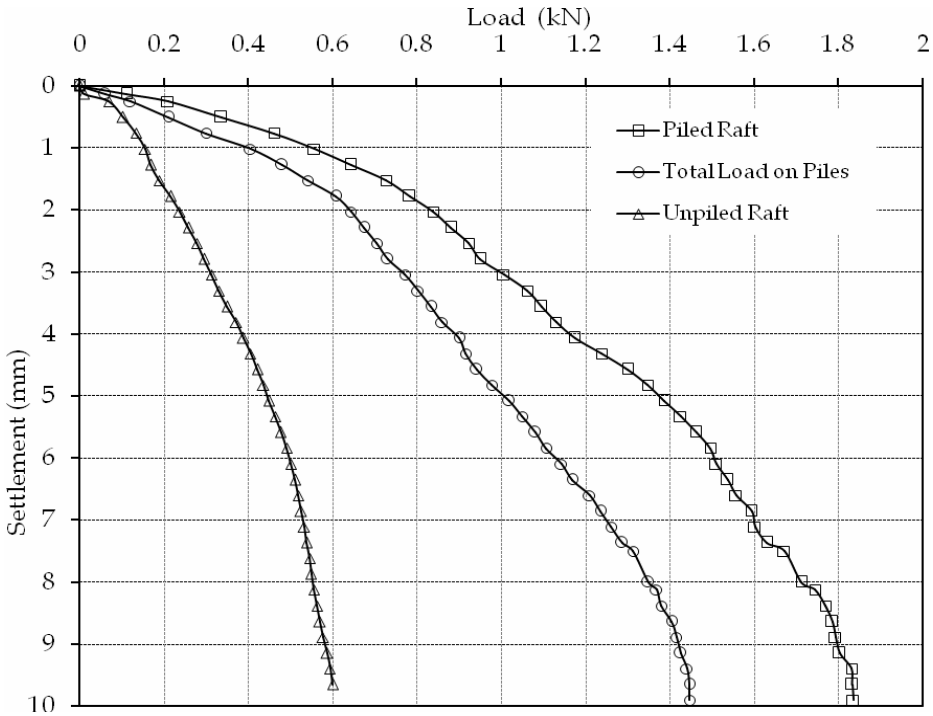


**Fig. (16)** Load – displacement curve for (**2x2**) piled raft, unpiled raft and total load on piles (L=200 mm and D=15 mm).

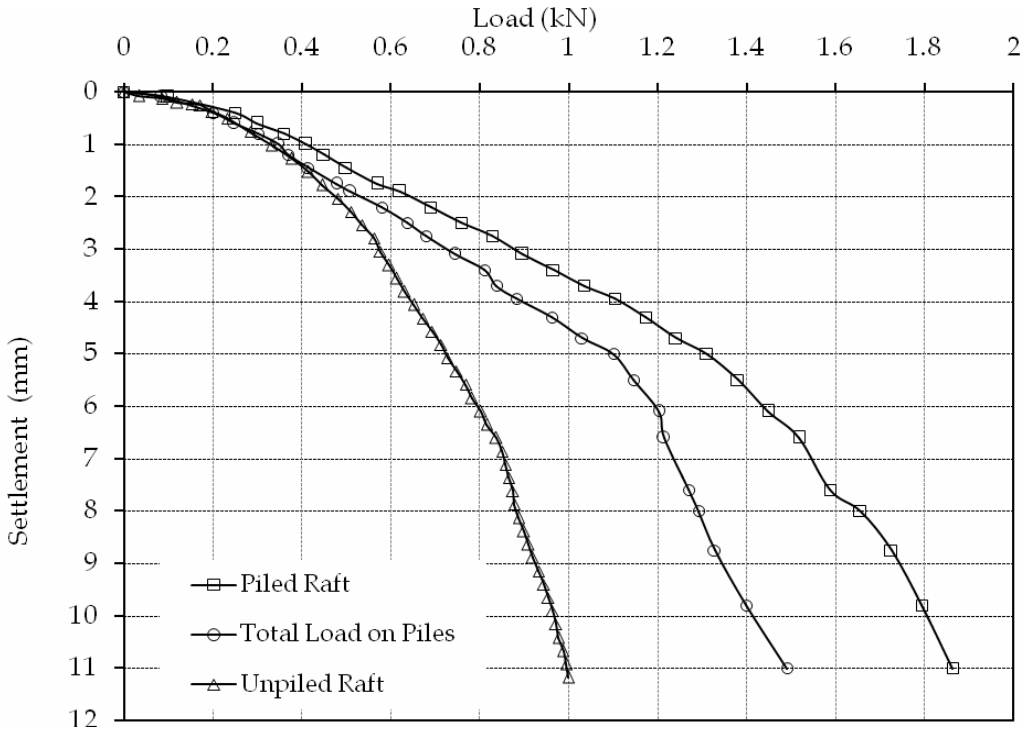


**Fig. (17)** Load – displacement curve for (**3x2**) piled raft, unpiled raft and total load on piles (L=200 mm, D=9 mm).

**Selection of Failure Criterion**

Several criteria have been proposed for defining the failure load of the piles. Some of these criteria are described by Fellenius (2006) as follows:

- **De Beer** in 1967 proposal. The bearing capacity is taken at break point of two intersecting straight lines of different slopes after plotting the load-settlement relationship in log-log plot. This break point represents failure.
- **Terzaghi** in 1947 proposal, where failure was defined as the load corresponding to dispalcment of 10% of the model footing width (or pile diameter ).
- **Tangent** proposal, in which definition of failure based on the intersection of the two tangents of load-settelment curve while the second is tangent to the lower flatter portion of the curve.
- **Chin** in1970 proposal, this method assumes that the load-settlement curve is hyperbolic in shape when the failure load is approached. Each load value is divided by its corresponding settlement value and the resulting value is plotted against the settlement, the plotted value fall on a straight line, so the inverse of the slope of this line is the Chin failure load

After examining the previous proposals and by inspection of the behavior of the load-settlement relation for the piles in the present work, it was found that the tangent proposal can be adopted in specifying the ultimate piled raft capacity. The piles carrying capacity for the studied groups with different diameters are shown in table (3)

By checking **Figures (8) to (17)**, it can be noted that the piles carrying capacity increases with the increase of the pile diameter for all the studied groups. The total carrying capacity of the piles relative to the total applied load increases also with the increase in the number of piles in the group, whereas the group of (3x2) recorded the maximum piles capacity with 79% of the total applied load.

**Effect of Raft Size and Thickness**

The experimental study included implicitly the testing of rafts (unpiled rafts) of different sizes and thicknesses to compare the results with those of the piled raft system. The aluminum plates used for modeling the rafts are relatively of high stiffness which yields a uniform distribution of load between piles. Unpiled rafts with dimensions similar to the rafts used with groups of piles to form the piled raft system were testes separately. The load settlement curves are shown in **Figure (18)** for rafts having a thickness of (5) mm.

To study the effect of raft sized, the pressure under the raft is plotted against the settlement, as shown in **Figure (18)**. The pressure under the raft of size (15x10 cm) was (64 $kN/m^2$) corresponding to a settlement of 10 mm, this value is 30% greater than the pressure under a raft of size (6x10 cm) and corresponding to the same settlement. The case of raft with size (6x15 cm) showed the lowest values of pressure under the raft, and this may be attributed its relatively narrow width.

**Table** (3) Piles capacity for the studied cases.

| Case | Pile Raft Capacity (kN) | Piles Capacity (kN) | % of Load Carried by Piles |
|---|---|---|---|
| (2x1) Group, L = 200 mm, D = 9 mm | 0.25 | 0.068 | 27 |
| (2x1) Group, L = 200 mm, D = 12 mm | 0.365 | 0.14 | 38 |
| (2x1) Group, L = 200 mm, D = 15 mm | 0.5 | 0.26 | 52 |
| (3x1) Group, L = 200 mm, D = 9 mm | 0.4 | 0.144 | 36 |
| (3x1) Group, L = 200 mm, D = 12 mm | 0.51 | 0.25 | 49 |
| (3x1) Group, L = 200 mm, D = 15 mm | 0.62 | 0.325 | 52 |
| (2x2) Group, L = 200 mm, D = 9 mm | 0.83 | 0.45 | 54 |
| (2x2) Group, L = 200 mm, D = 12 mm | 1.15 | 0.78 | 68 |
| (2x2) Group, L = 200 mm, D = 15 mm | 1.6 | 1.25 | 78 |
| (3x2) Group, L = 200 mm, D = 9 mm | 1.62 | 1.275 | 79 |

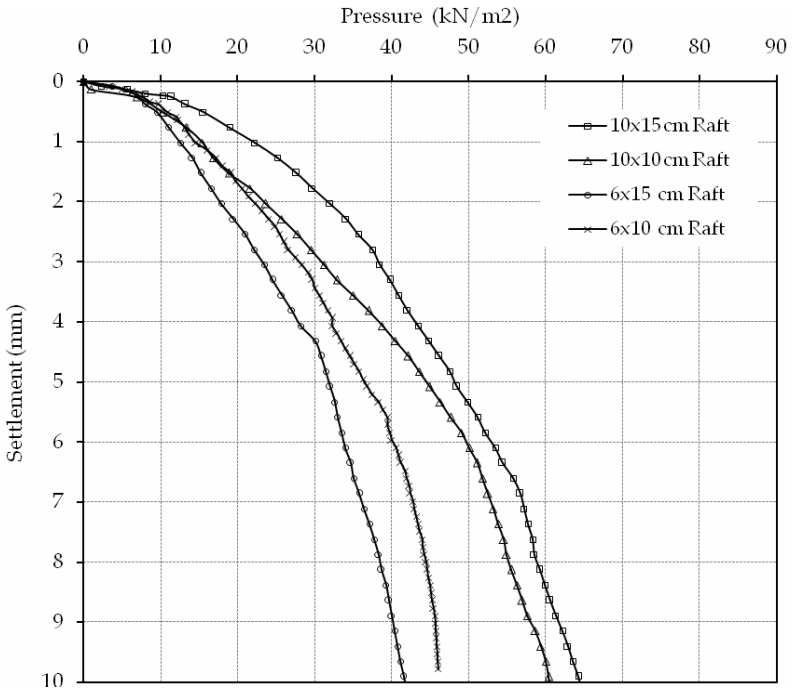


**Fig. (18),** Load – displacement of unpiled rafts of different sizes ($t_r$ = 5 mm).

The effect of raft thickness is also studied for the case of piled raft system, a thickness of (2.5) mm tested with (2x2) group of piles, for L= (200) mm and D= (12) mm.

The results of load settlement curve and the load carrying capacity of piles are shown in **Figure (19)** in which the unpiled raft with the same thickness is also shown. The total bearing capacity of piled raft system is not much affected by the raft thickness, while the total load carried by piles is slightly reduced. The percent of load carried by piles is plotted against the raft thickness in **Figure (20)**.

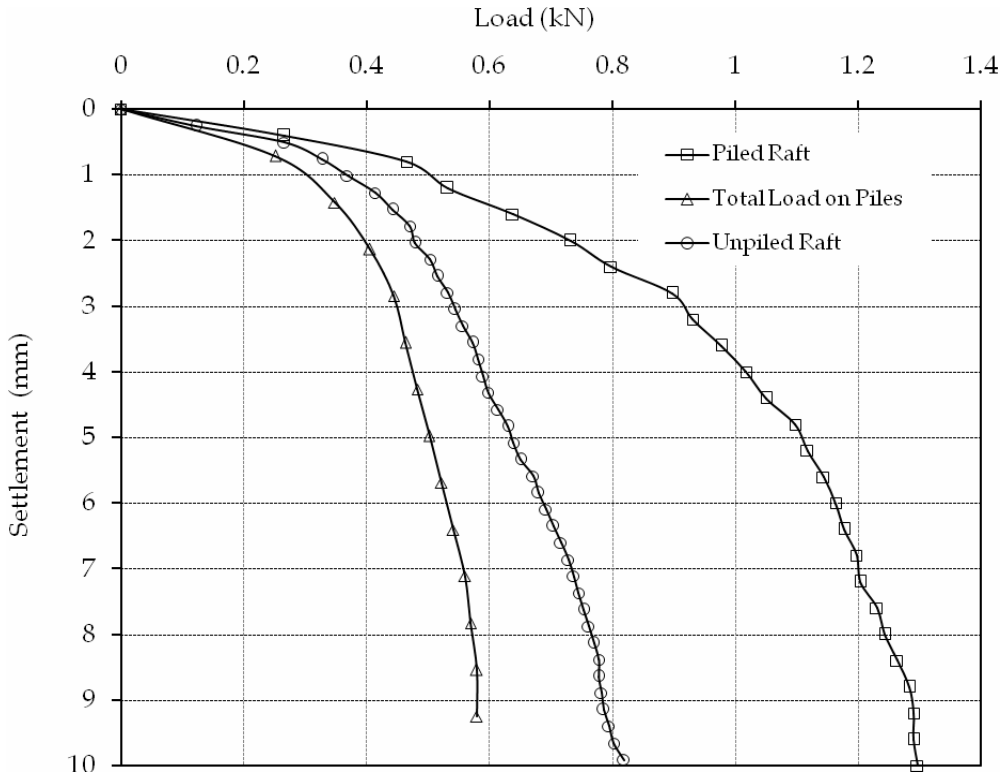


**Fig. (19)** Load – displacement curve for (2x2) piled raft, unpiled raft and total load on piles (L=200 mm, D=12mm, and $t_r$=2.5 mm).

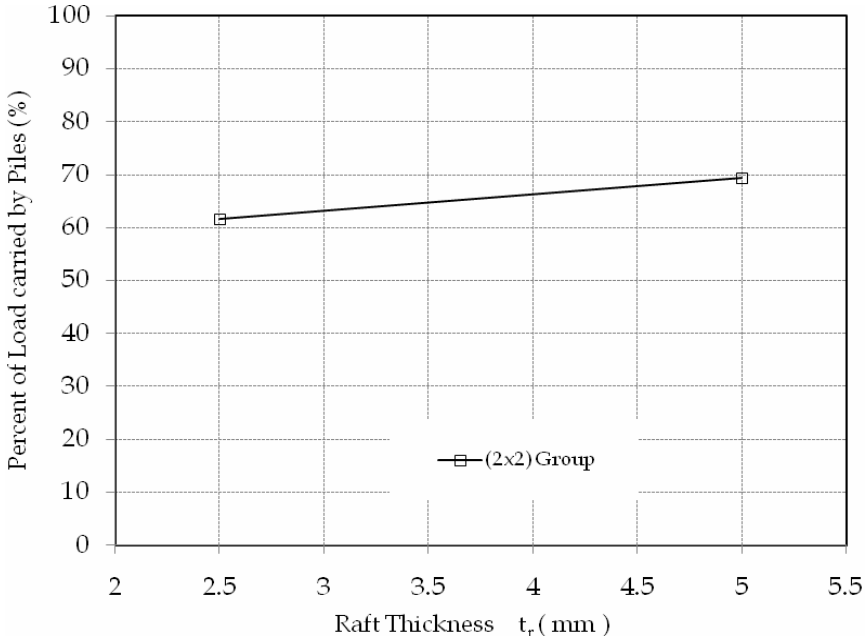


**Fig. (20),** Percent of load carried by piles for (2x2) group of piles (L=200 mm, D=12 mm) with raft thickness.

## CONCLUSIONS

The experimental modeling implemented in this paper yielded the following conclusions:

1. The load carrying capacity of the unpiled raft increases with the increase of the size, while the raft thickness slightly affects the load carrying capacity. For the piled raft model, the total carrying capacity of the model increased with the increase of raft size, number of piles in the group, length of piles, and diameter of piles.
2. The percentage of the load carried by piles to the total applied load of the groups (2x1, 3x1, 2x2, 3x2) with raft thickness of 5 mm, pile diameter of 9 mm, and pile length of 200 mm was 28% , 38% , 56% , 79% , respectively. The percent of the load carried by piles increases with the increase of number of piles.

## REFERENCES


- Al-Jebouri, J. M. (1986), "Bearing Capacity of Footing on Reinforced Sand" M.Sc. Thesis, University of Baghdad, Iraq.
- Bieganousky, W. N. and Marcuson, W. F. (1976),"Uniform Placement of Sand", Journal of Geotechnical Engineering Div., ASCE, Vol. 102, No. GT.3,pp.229-233.
- Burland, J.B., Broms, B.B. and de Mello, V.F.B. (1977), "Behaviour of Foundations and Structures", Proc. 9th ICSMFE, Tokyo, Vol.2, pp. 495-546.
- Cox, W. R., Dixon, D. A., and Murphy, B. S. (1984), "Lateral-Load Tests on 25.4-mm (1-in.) Diameter Piles in Very Soft Clay in Side-by-Side and in-Line Groups" Laterally Loaded Deep Foundations: Analysis and Performance, ASTM STP 835, 122-139.

- 
- Davis, E. H. and Poulos, H. G. (1972), Rate of Settlement under Two-and Three-Dimensional Conditions, Geotechnique, Vol.22, No.1, pp. 95-114.
- de Sanctis L., and Mandolini A., (2006), "Bearing Capacity of Piled Rafts on Soft Clay Soils", Journal of Geotechnical and Geoenvironmental Engineering, ASCE, Vol. 132, No. 12, pp. 1600-1610.
- Fellenius, B. H., (2006), "Basics of Foundation Design:, Electronic Edition. www.Fellenius.net, 275 p.
- Hartman, F. and Jahn, P. (2001), "Boundary Element Analysis of Raft Foundations on Piles", Meccanica Vol. 3, pp. 351–366, Kluwer Academic Publishers. Netherlands.
- Hooper, J.A., (1973), "Observations on the Behavior of a Piled Raft Foundation in London Clay", Proceeding of Institution of Civil Engineers, Vol.55, No.2, pp. 855-877.
- Jawad, W. F. (2009)," Improvement of Loose Sand Using Geogrids to Support Footing Subjected to Eccentric loads", M.Sc. Thesis, University of Baghdad, Iraq.
- Katzenbach, R. and Reul, O. (1997), "Design and Performance of Piled Rafts", Proceeding XIVth ICSMFE, Hamburg Vol. 4, pp. 2253-2256.
- Model 3800 Instruction Manual, (2002), "Wide Range Strain Indicator", USA, www.vishaymg.com.
- Mokwa, R. L. (1999), "Investigation of the Resistance of Pile Caps to Lateral Loading", Ph.D. Thesis, Virginia Polytechnic Institute and State University, USA.
- Prakoso, W.A. and Kulhawy, F.H., (2001), "Contribution to Piled Raft Foundation Design", Journal of Geotechnical and Geoenvironmental Engineering, ASCE, Vol.127, No.1, pp.17-24.
- Reul, O. and Randolph, M. F., (2003), "Piled Rafts in Overconsolidated Clay: Comparison of in Situ Measurements and Numerical Analysis", Geotechnique, Vol. 53, No. 3, pp. 301-315.
- Turner, J. P. and Kulhawy, F. H. (1987), "Experimental Analysis of Drilled Foundations Subjected to Repeated Axial Loads Under Drained Conditions", Report EL-5325, Electric Power Research Institute, Palo Alto, California.
- Zeevaert, L. (1957) "Compensated Friction-pile Foundation to Reduce the Settlement of Buildings on Highly Compressible Volcanic Clay of Mexico City", Proc. 4th ICSMFE, London, V.2.